Hindawi
International Journal of Photoenergy
Volume 2018, Article ID 8478240, 8 pages
https://doi.org/10.1155/2018/8478240

Research Article

Synthesis and Characterization of TiO_2/SiO_2 Monoliths as Photocatalysts on Methanol Oxidation

Rigoberto Regalado-Raya,[1] Rubí Romero-Romero,[2] Osmín Avilés-García,[1] and Jaime Espino-Valencia[1]

[1]*Facultad de Ingeniería Química, Universidad Michoacana de San Nicolás de Hidalgo, Edif. V1, Ciudad Universitaria, 58060 Morelia, Michoacán, Mexico*
[2]*km 14.5 Carretera Toluca-Atlacomulco, San Cayetano, Piedras Blancas, Centro Conjunto de Investigación en Química Sustentable UAEMéx-UNAM, Toluca, Estado de México, Mexico*

Correspondence should be addressed to Jaime Espino-Valencia; jespinova@yahoo.com.mx

Received 21 July 2017; Revised 6 November 2017; Accepted 13 March 2018; Published 23 September 2018

Academic Editor: Juan M. Rodriguez

Photocatalytic materials based on silica-titania (SiO_2-TiO_2) were synthesized by sol-gel and dip-coating method. TEOS and titanium butoxide were used as precursors of the silica-titania, respectively. A thin film with anatase phase was obtained on the surface of the support. The effect of variables as dispersion mechanism, immersion time, and number of treatment cycles were studied. The materials were characterized using X-ray diffraction, scanning electron microscopy, energy dispersion scanning, and N_2 adsorption-desorption. The highest crystallinity of TiO_2 on silica, high specific surface area in TiO_2-SiO_2 materials, and thin film formation were obtained by using a stirring plate and minimum immersion time. The so synthesized catalyst allowed the production of formaldehyde from the photocatalyzed methanol oxidation in a packed-bed reactor.

1. Introduction

Among the advanced oxidation processes (AOPs), heterogeneous photocatalysis has been widely applied in the degradation of organic compounds, hydrogen production from water, reduction of heavy metals, and selective oxidation reactions [1–4]. Selective oxidation of alcohols to aldehydes by photocatalysis is an attractive route because it can be carried out under mild conditions (room temperature, atmospheric pressure, and neutral pH) [5, 6]; particularly, formaldehyde is a highly important intermediate compound in the chemical industry because of its use in the synthesis of adhesives, fertilizers, pyridines, drugs, polyols, and dyes among others [7, 8]. The industrial production of formaldehyde is performed from the oxidation and dehydrogenation of methanol with iron molybdate and silver catalysts, respectively [9, 10].

The most studied semiconductor in the field of heterogeneous photocatalysis is titanium dioxide (TiO_2) due to its high oxidative capacity, nontoxicity, low cost, high chemical and physical stability, corrosion resistance, and chemical inertness [11, 12]. TiO_2 has been widely used in both powders and thin films [13, 14]. When it is used as suspended particles, a separation step such as filtration or centrifugation is required at the end of the process. For this reason, the immobilization of the particles in an appropriate substrate has attracted great interest [15].

There are several methods for the preparation of TiO_2 thin films, and the physicochemical properties strongly depend on the selected method [16–19]. Among all the techniques, the dip-coating sol-gel method is the most widely used because of its good homogeneity, simplicity, low cost, and low temperature during the process [20]. On the other hand, the nature and type of substrate should not be left

aside. Amorphous SiO_2 has shown to be an excellent support due to its mechanical properties, good adsorption capacity, and high surface area [21, 22].

This work aims to elucidate the effect on morphological, textural, and structural properties of three important variables involved in the synthesis of TiO_2 coated SiO_2 monoliths. These variables are the mechanism to disperse Ti alkoxide species in an appropriate medium allowing the hydrolysis-condensation processes, dipping time, and number of coating cycles (dip + drying + calcination). In order to evaluate the photocatalytic activity of the synthesized catalysts, the photooxidation of methanol was carried out in a bench-scale continuous-flow packed-bed reactor. This reaction was elected because of its industrial importance and because it is a consecutive reaction, whose selectivity towards intermediate compounds may help to prove the application of TiO_2 in selective oxidation processes instead of the organic compounds mineralization. This process could offer the advantage being performed at mild temperature and pressure conditions unlike other existing processes that occur at relatively high temperatures.

2. Experimental

2.1. Preparation of SiO_2 Monoliths. Silica dioxide monoliths were synthesized by sol-gel method. The synthesis of the silica support was performed using tetraethyl orthosilicate (TEOS) $[Si(OC_2H_5)_4]$ as alkoxide precursor of the Si sol.

First, the ethanol was added into a beaker and it was maintained under continuous stirring until the temperature reached 60°C. At this point, alkoxide was added and mixed into the beaker for 15 min. After this time, a water and nitric acid solution (1 : 0.0012 molar ratio) was added and the mixture was kept under stirring and keeping the temperature constant for one hour. The molar ratio of water : ethanol : TEOS was of 16 : 4 : 1, respectively.

After that, 2.5 ml of the resulting sol were poured into one container to begin the aging process. This was repeated several times to obtain various monoliths. The container lids were previously drilled to allow solvent diffusion. During this step, alkoxide groups are removed by acid- or base-catalyzed hydrolysis reactions, and link networks O-Si-O are formed in subsequent condensation reactions involving hydroxyl groups [23, 24]. Depending upon the water : alkoxide molar ratio *R*, pH, temperature, and solvent, condensation leads to different polymeric structures such as linear, entangled chains, clusters, and colloidal particles [25].

The obtained monoliths were then dried from room temperature to 100°C during 14 hours with a slow heating profile to eliminate the solvent. The drying was performed in an Isotemp Vacuum Oven programmable stove model 282 A. The drying treatment was slow to lead the formation of open pores. The drying profile was as follows: 1 h at 40°C, 2.5 h at 50°C, 13 h at 60°C, 2.5 h at 70°C, 3.5 h at 80°C, 2.5 h at 90°C, and 27 h at 100°C. This procedure was performed in order to keep the structure, since a fast drying profile could cause a structure collapse causing cracking of the monolith.

Finally, to provide the monoliths with the appropriate structural and mechanical properties, they were calcined from room temperature (25°C) to 550°C for 6 h at a heating rate of 2.5°C/min using a Jelrus muffle with 2 steps. Amorphous silica compounds without a defined crystalline phase are found at this temperature.

2.2. TiO_2 Synthesis. Ethanol, water, titanium butoxide, and diethanolamine (basic catalyst) were used to obtain Ti sols via sol-gel method. Titanium butoxide ($Ti[O(CH_2)_3CH_3]_4$) was dispersed in the ethanol. Immediately, a diethanolamine and water solution was dropped into the volume. It is necessary to maintain a 1 : 1 alkoxide : water molar ratio. Once the solution addition was completed, the agitation was maintained for two hours. After this time, the solution was aged for further two hours without any stirring. Diethanolamine was elected because of its low reactivity during sol-gel process, this makes the hydrolysis reactions slow by favoring the thin film formation [26].

Finally, SiO_2 monoliths were immersed into the Ti sol obtained. In this process, the studied variables were the dispersion mechanism (mechanic or ultrasound) and the residence time into the Ti sol. For the former, a stirring plate and an ultrasonic cleaner were utilized as agitation media. Regarding residence time in the Ti sol, this variable was studied at three levels (half, one, and three hours) for each stirring medium. The number of cycles (immersion-drying-calcination) was also studied in order to establish its relationship with the amount of titania on SiO_2.

The monoliths coated with titanium species were dried at room temperature for 24 h and calcined under an air flow at 550°C for 5 hours.

2.3. Catalysts Characterization. A Bruker Advance 8 diffractometer was employed to carry out the X-ray diffraction analysis and determine the presence of anatase in the synthesized catalysts. The patterns were obtained using CuKα radiation at 20 kV and 20 mA. Data were collected over 2θ range of 5–50° with a step of 0.5°/min.

A JEOL JSM-6510LV electron microscope coupled with an energy dispersive X-ray spectrometer was employed to observe the surface morphology of the prepared catalysts and to perform elemental analysis of the catalysts.

Autosorb-1 Quantachrome sorption equipment was employed to determine the specific surface area and average pore diameter of the synthesized samples by using liquid nitrogen (77 K). The pore size distributions and the specific surface areas of the materials were estimated by Dubinin-Astakhov (DA) and Brunauer Emmett–Teller (BET) methodologies, respectively.

2.4. Bench-Scale Photocatalytic Reactor. The photooxidation of methanol was performed using a bench-scale continuous packed-bed reactor. An eight-watt UV lamp emitting 254 nm waves was placed right in the center of the reactor. 30 monoliths constituted the catalytic bed. Compressed air was used as carrier gas to help methanol to flow through the packed-bed reactor. The air flow was constant at 50 ml/min. The methanol liquid was heated at 65°C in order to vaporize it. The reactor set-up is depicted in Figure 1.

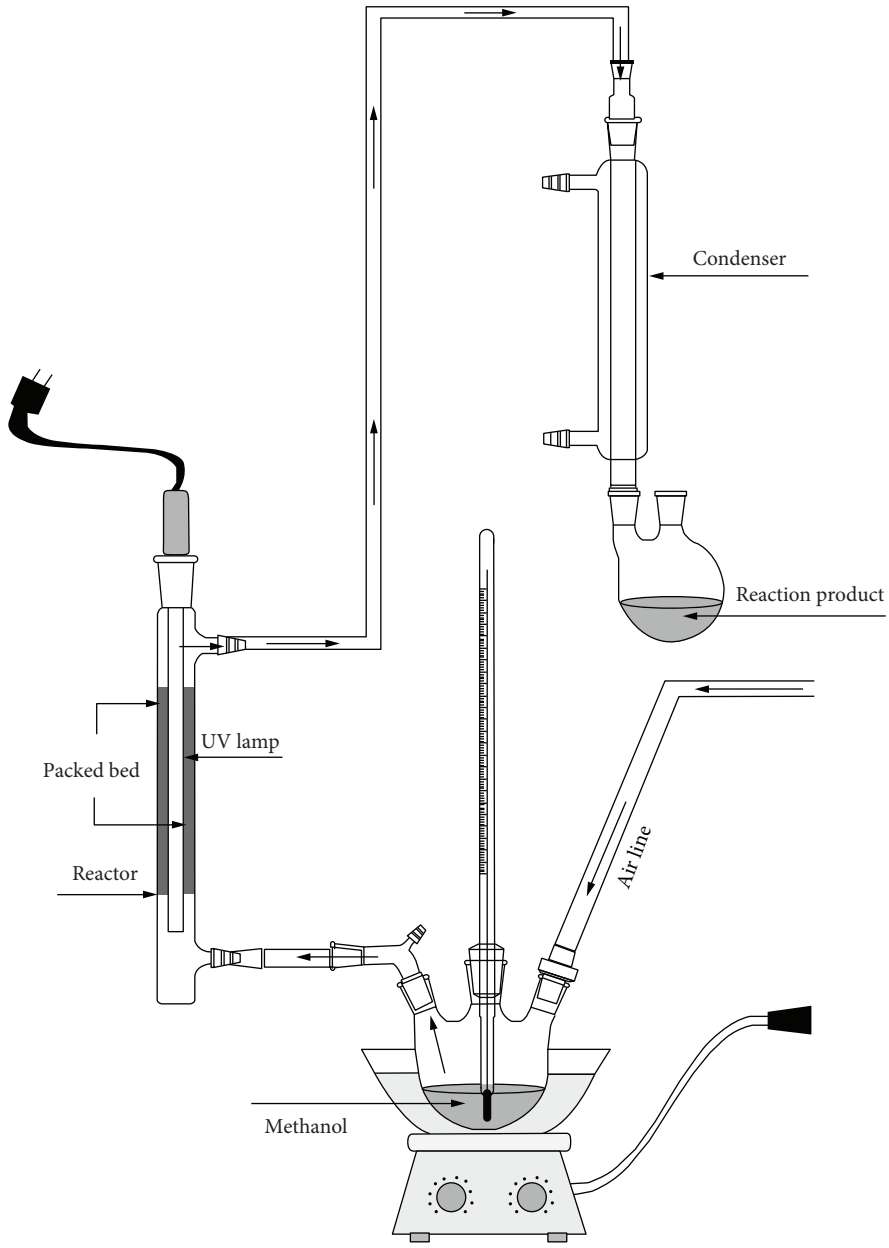

Figure 1: Bench-scale photocatalytic reactor set-up.

Identification of formaldehyde by photooxidation of methanol was carried out according to the following methodology: a proper container with a 2,4-dinitrophenylhydrazine (2,4-dnph) solution was placed instead of the condenser (see Figure 1), in such a way that the exit stream was directly bubbled into the solution. This was conducted with all synthesized materials. If there was formaldehyde in such a stream, then a precipitate was observed. This precipitate was the 2,4-dinitrophenylhydrazone, which is the product of the reaction between the 2,4-dnph and the aldehyde as depicted in Figure 2 [27].

The 2,4-dnph solution was prepared as follows: 2 ml of concentrated sulfuric acid was mixed under stirring with 0.4 gr of 2,4-dnph and 3 ml of water until total dissolution appears. At this point, 10 ml of ethanol at 95% are added to the solution.

The quantitative analysis of formaldehyde after photooxidation of methanol was verified by collecting the condensed reaction product in a container at 4°C and analyzed in a Varian GC 3800 using a 52 CP WAX column (30 m × 0.320 mm).

3. Results and Discussion

SiO_2 monoliths with a diameter of 15 mm and thickness of 1 mm approximately were obtained following the methodology described in the previous section. Figure 3 shows such monoliths. It can be observed that they are totally transparent. This is expected to allow an excellent light transmittance

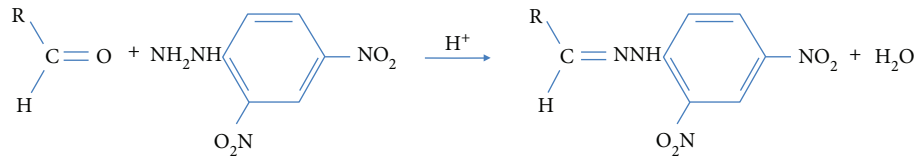

Figure 2: 2,4-Dinitrophenylhydrazine general reaction with aldehyde functional groups.

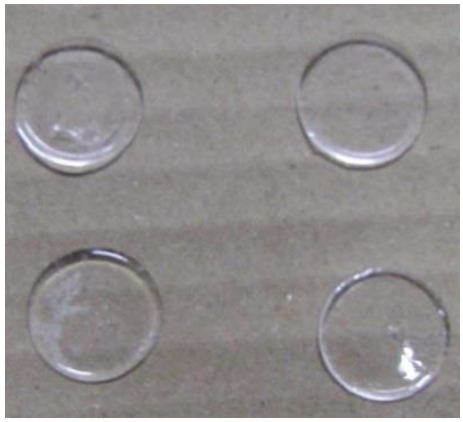

Figure 3: SiO_2 monoliths obtained by sol-gel technique.

Table 1: Nomenclature of synthesized materials (B by ultrasound bath and P by stirring plate).

Sample name	Number of immersion-drying-calcination cycles	Immersion time (hours)
3ST12B	3	1/2
3ST12P	3	1/2
3ST1B	3	1
3ST1P	3	1
3ST3B	3	3
3ST3P	3	3
4ST1P	4	1

and an appropriated use in photocatalytic reactions using UV light.

In total, 8 samples were characterized in order to decide at what conditions the monoliths for the methanol photooxidation should be synthesized. From the 8 monoliths, 7 were coated with TiO_2 while the left one was only SiO_2. The nomenclature used to name the samples is explained in Table 1.

Figure 4 shows the diffraction patterns with respect to the agitation mechanism and number of immersion-drying-calcination cycles. The obtained crystalline phase is mainly anatase, and this is expected because of the calcination temperature (550°C) [28]. Usually, when the calcination temperature is increased to more than 550°C, the anatase phase is observed to gradually change into a rutile phase with a larger particle size that results unfavorable for photocatalytic degradation reactions [29].

The average crystallite size of samples was estimated using the Scherrer's equation through the full width at half maximum of the anatase (101) peak (see Table 2). Based on these results, it can be observed that the agitation mechanism has a significant effect on crystallinity since the monoliths coated in the ultrasound bath exhibit the smallest crystalline size (Figure 4(d)) than that of prepared with mechanical stirring (Figure 4(c)) to the same number of cycles (3 cycles) and residence time in the sol (3 hours). The diffraction pattern for commercial Degussa P-25 is included on the top right corner of Figure 4 for reference purposes. It can also be observed that the obtained SiO_2 is amorphous (Figure 4(e)). As can be seen in Table 2, the number of treatment cycles decreases crystal growth. In addition, the increase in immersion time for samples with 3 treatment cycles decreased the crystallinity. The sample with the largest crystalline size corresponds to 3 treatment cycles and half an hour of immersion (sample 3ST12P). It is worth mentioning that more than 3 cycles were unsuccessfully attempted since monoliths got broken, with the exception of those with 1 hour immersion time. In this case, monoliths did not stand the fifth cycle.

Regarding samples 3ST1B and 3ST12B, these were discarded because the ultrasound influenced the structure to an extent that the SiO_2 monolith was broken. This may be ascribed to the vibrational movements caused by ultrasonic, causing the structure to become weaker. This is a consequence of the immersion under ultrasound presence during TiO_2/SiO_2 monoliths preparation as well as the decrease in crystallinity.

Figure 5 (3ST12P sample) shows the surface morphology of TiO_2 film obtained after 3 cycles of immersion-drying-calcination treatments. The residence time was half an hour for each of the immersion processes. The film exhibits a homogeneous morphology with a lineal growing up with almost totally flat surface. The EDS analysis shows the Ti presence. Figure 6 (3ST1P sample) presents the surface of the TiO_2 film obtained after 3 cycles of immersion-heating-calcination treatments and one hour of residence time for each immersion process.

Figure 7 (3ST3P sample) illustrates the characteristic morphology of a TiO_2 film after 3 treatment cycles and 3 hours of immersion under mechanical stirring. The comparison of Figures 7 and 5 make it clear that the amount of material deposited on the surface increases with immersion time. This increase is not related to the crystalline growth of anatase on the surface as has been evidenced by XRD analysis. The clusters presented in Figure 7 can be ascribed to the time given to the monolith in the sol where hydrolysis and condensation reactions are occurring, so the longer the immersion time, the larger the agglomerate.

By comparing Figures 5–7, it can be observed that the residence time has a significant effect on the morphology of

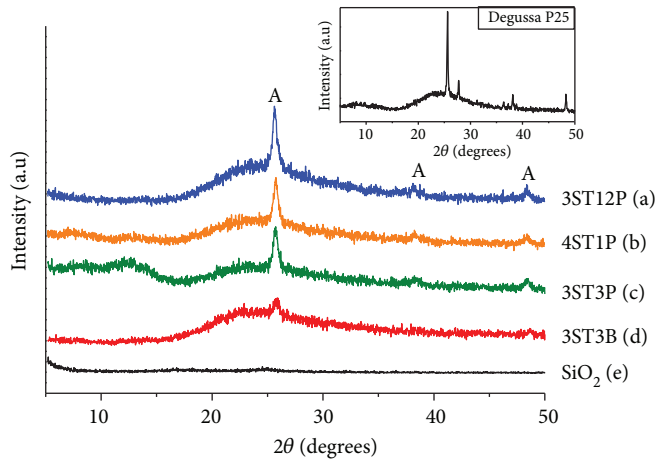

Figure 4: XRD patterns of TiO_2/SiO_2 and pure SiO_2 samples.

Table 2: Average crystallite size of the synthesized materials in Figure 4.

Sample	Average crystallite size (nm)
3ST12P	19.4
4ST1P	17.0
3ST3P	16.3
3ST3B	13.5

the coating. A time higher than half an hour (Figures 6 and 7) promotes the appearance of microcracks, and therefore the film loses homogeneity. These microcracks may be ascribed to a stress effect during the drying-calcination treatment due to thermal shrinkage and expansion phenomena. The stress is caused by chemical reactions during the drying and thermal expansion coefficients difference between the support (5×10^{-7}°C) and TiO_2 film ($2.1\text{-}2.8 \times 10^{-6}$°C) [30]. It seems that the effect of this phenomenon becomes stronger when the amount of TiO_2 increases due to the drying and calcination process. The crystallinity of the sample shown in Figure 5 may be related to the absence of cracking since with the growth of the crystal and densification of the film, the compressive stresses are reduced.

Figure 8 (4ST1P sample) shows an image of a TiO_2 film after 4 treatment cycles and 1 hour of immersion under mechanical stirring. The comparison of the EDS analysis of this with that in Figure 6 confirms that the amount of TiO_2 is a direct function of the number of dip coating/heat treatment cycles and that the extent and frequency of the microcracks increase with the number of cycles [31, 32].

The final percentage in weight gained of TiO_2 by the SiO_2 monoliths is shown in Table 3. It can be observed that the increase in immersion time (samples 3ST12P and 3ST1P) favors the amount of TiO_2 deposited on the monoliths. On the other hand, the increase in the number of treatment cycles (samples 3ST1P and 4ST1P) decreases the final percentage of weight gained of TiO_2.

Table 4 shows the specific surface area and average pore diameter of synthesized materials. All samples presented type I isotherms and average pore sizes of 18 Å, which according to the IUPAC classification corresponds to materials with microporous texture. It can be seen that the pure SiO_2 monolith presented the highest surface area (339 m^2/g). As the immersion time of the monoliths increases, the surface area decreases by about 50% (3ST3P sample). This decrease can be attributed to the amount of TiO_2 on the SiO_2 surface. Although the surface area decreases, the pore size distribution and the mean diameter are maintained.

It can be said that the synthesis conditions in which better crystallinity of the anatase phase is obtained; the highest specific surface area as well as a better uniformity of the formed film are with half an hour immersion, 3 cycles and stirring plate as dispersion mechanism. Therefore, these conditions were used to synthesize 30 monoliths to pack the bed reactor in order to perform the photocatalytic oxidation of methanol.

The minimum air flow rate to carry the methanol gas through the reactor was established as 50 ml/min. Two sets of experiments by triplicate were performed; one set without catalyst and the other one with the catalyst. In the former case, no formaldehyde was detected by the employed analysis method (2,4-dnph), and therefore the production of formaldehyde by photolysis was discarded. In the latter set of experiments, formaldehyde was identified. The analytical technique for the qualitative analysis of formaldehyde with a 2,4-dnph solution was carried out. The formation of micelles as precipitates is due to the formation of 2,4-dinitrophenylhydrazone indicating the presence of formaldehyde during the photocatalytic reaction. A precipitate indicating the presence of the aldehyde was only observed with the material 3ST12P. This does not mean that the other materials did not have photoactivity but that this could be so high that total methanol oxidation rather than selective oxidation was attained. To determine the amount of formaldehyde formed during photooxidation of methanol, the first condensed reaction product was evaluated by gas chromatography (GC). The final concentration of produced formaldehyde corresponds to a value of 457 micromol/L (13.7 mg/L). This result is superior to those obtained with other titania-silica systems [33].

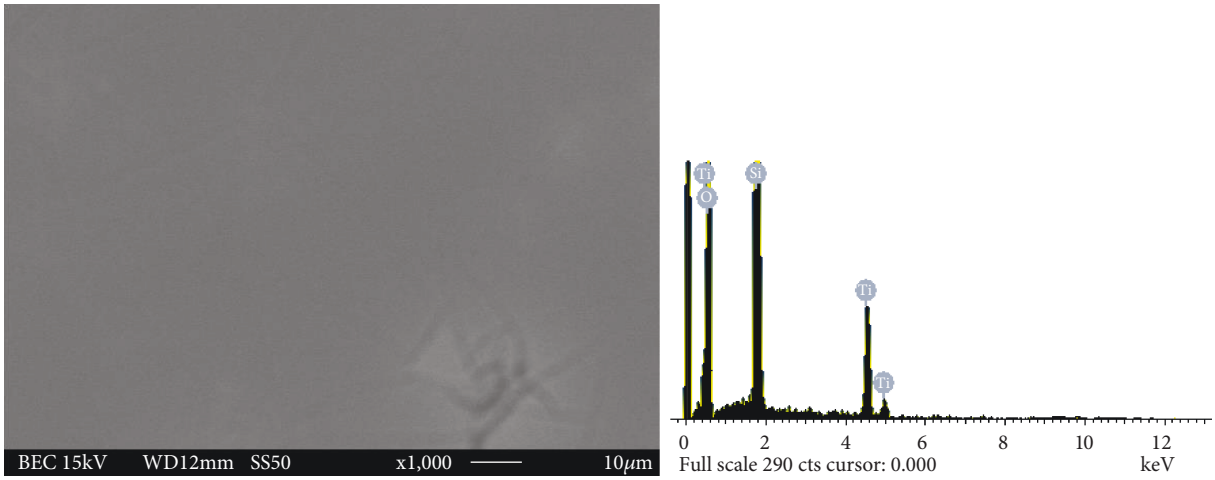

Figure 5: SEM image of TiO_2 film morphology obtained after 3 treatment cycles using a stirring plate and half an hour of immersion.

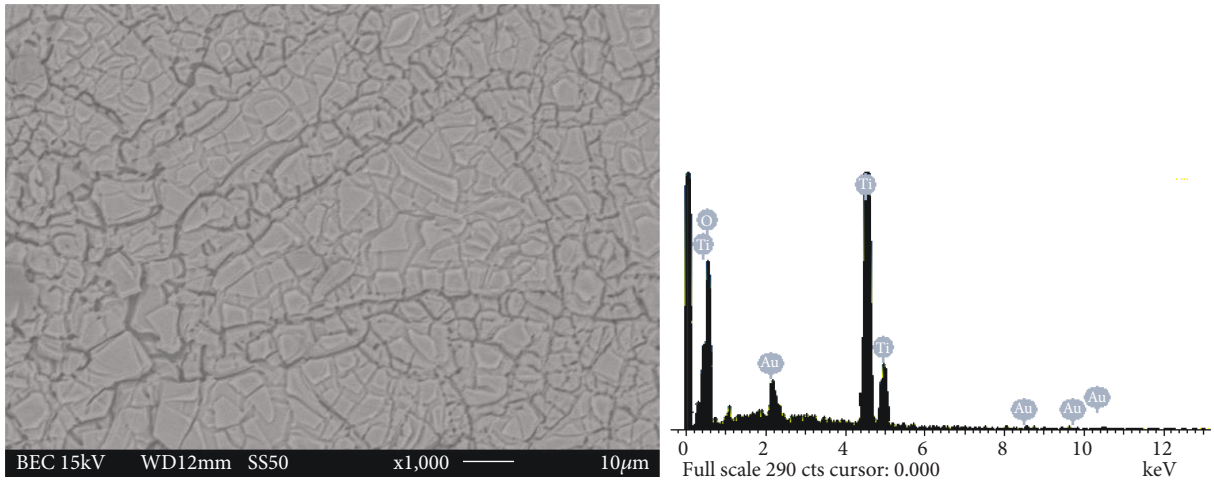

Figure 6: SEM image after 3 treatment cycles using stirring plate and 1 hour of immersion.

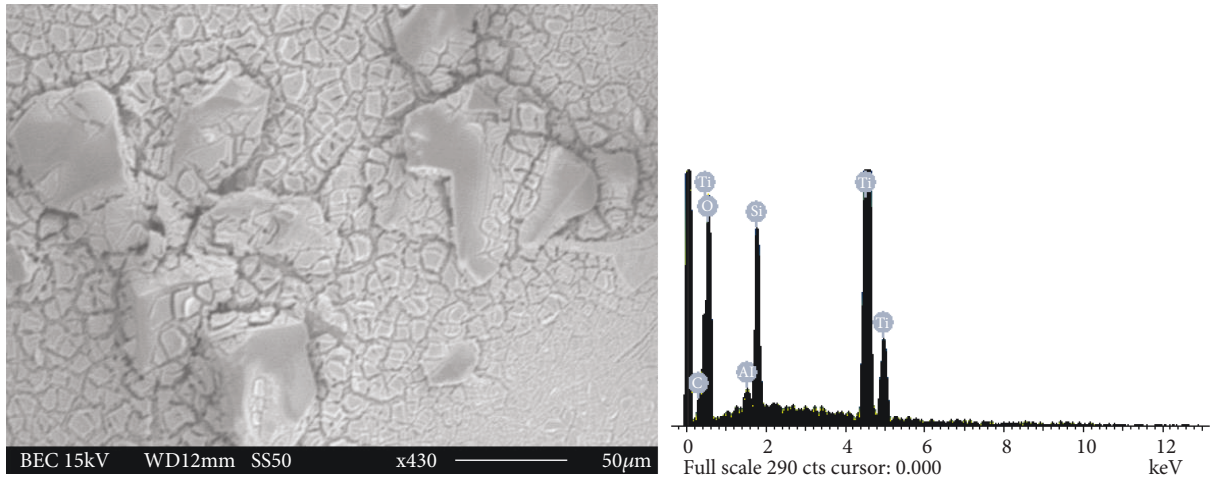

Figure 7: SEM image after 3 treatment cycles using stirring plate and 3 hours of immersion.

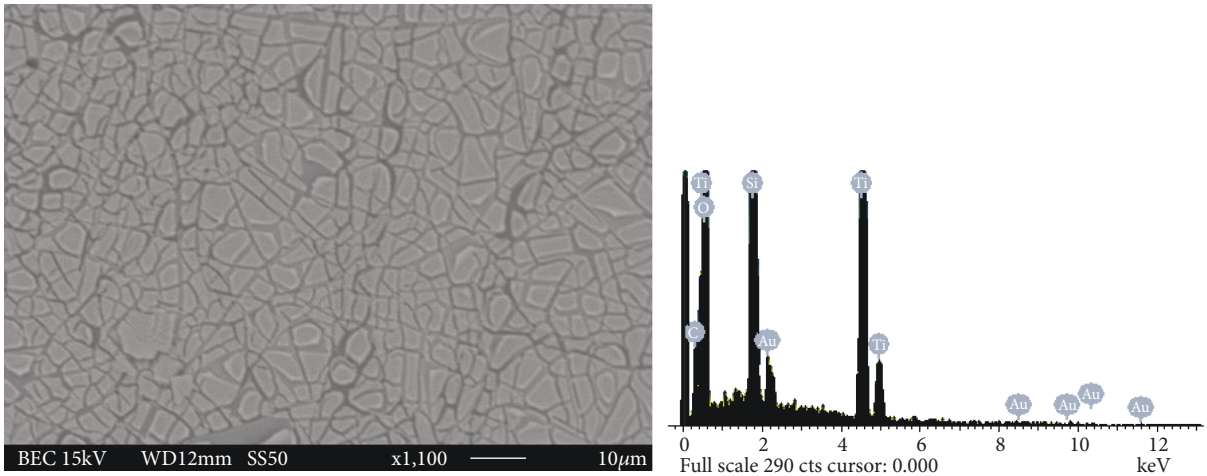

Figure 8: SEM image of TiO_2 film after 4 treatment cycles and 1 hour of immersion under mechanical stirring.

Table 3: Final percentage in weight gained of TiO_2 on the SiO_2 monoliths.

Sample	Percentage in weight gained of TiO_2 (%)
3ST12P	14.3
3ST1P	18.5
4ST1P	17.4

Table 4: Specific surface area and average pore size of the synthesized materials.

Sample	Specific surface area (m^2 g^{-1})	Average pore size (Å)
SiO_2	339	18
3ST12P	241	18
3ST1P	210	18
3ST3P	170	18
4ST1P	240	18

4. Conclusions

SiO_2 monoliths coated with thin films of TiO_2 anatase phase were successfully prepared by using a dip-coating sol-gel method. The dispersion mechanism, the immersion time, and the number of dip-coating cycles of the SiO_2 monoliths into the Ti sol were found to affect both the morphology and crystallinity of the TiO_2 deposit. SiO_2 monoliths coated with crackle-free TiO_2 films were obtained after three dip-coating cycles, with a dip time of 30 minutes. It can also be concluded that mechanical stirring should be preferred over ultrasound dispersion since the former favors the structural stability of the monolith and increases the film crystallinity, while the ultrasound dispersion method leads to monolithic structure breakage and also increases film crackles. Immersion time diminished both TiO_2 film and homogeneity. Immersion time and number of cycles also affect the surface area and deposit crystallinity. The surface area of the SiO_2-TiO_2 materials was decreased when the immersion time increased, which is related to the amount of TiO_2 on the SiO_2 surface. The highest anatase phase crystallinity and specific surface area were obtained after 3 dip-coating cycles and half an hour of immersion under mechanical stirring. Under these preparation conditions, the attained surface area was 241 m^2/g and the crystallite size was 19.4 nm. The weight percentage gained by SiO_2 monoliths was 14.3% (TiO_2 film).

A formaldehyde concentration of 13.7 mg/L was attained at mild conditions of pressure and temperature in a continuous flow reactor packed with SiO_2 monoliths coated with TiO_2 anatase films prepared with 3 dip-coating cycles and 0.5 hours of immersion time.

Conflicts of Interest

The authors declare that there is no conflict of interests.

Acknowledgments

The authors are grateful to UAEMex for the financial support through project 4373/2017/CI and to CONACYT (project 269093). R. Regalado would like to thank CONACYT for the financial support and to CCIQS from UAEM for the granted support.

References

[1] Z. Li, S. Cong, and Y. Xu, "Brookite vs anatase TiO_2 in the photocatalytic activity for organic degradation in water," *ACS Catalysis*, vol. 4, no. 9, pp. 3273–3280, 2014.

[2] H. Park, C. D. Vecitis, W. Choi, O. Weres, and M. R. Hoffmann, "Solar-powered production of molecular hydrogen from water," *The Journal of Physical Chemistry C*, vol. 112, no. 4, pp. 885–889, 2008.

[3] J. Wang, Z. Bian, J. Zhu, and H. Li, "Ordered mesoporous TiO_2 with exposed (001) facets and enhanced activity in photocatalytic selective oxidation of alcohols," *Journal of Materials Chemistry A*, vol. 1, no. 4, pp. 1296–1302, 2013.

[4] M. Pera-Titus, V. García-Molina, M. A. Baños, J. Giménez, and S. Esplugas, "Degradation of chlorophenols by means of

advanced oxidation processes: a general review," *Applied Catalysis B: Environmental*, vol. 47, no. 4, pp. 219–256, 2004.

[5] A. Tanaka, K. Hashimoto, and H. Kominami, "Selective photocatalytic oxidation of aromatic alcohols to aldehydes in an aqueous suspension of gold nanoparticles supported on cerium(iv) oxide under irradiation of green light," *Chemical Communications*, vol. 47, no. 37, pp. 10446–10448, 2011.

[6] Y. Zhang, Z. R. Tang, X. Fu, and Y. J. Xu, "Engineering the unique 2D mat of graphene to achieve graphene-TiO_2 nanocomposite for photocatalytic selective transformation: what advantage does graphene have over its forebear carbon Nanotube?," *ACS Nano*, vol. 5, no. 9, pp. 7426–7435, 2011.

[7] G. Reuss, W. Disteldorf, O. Grundler, and A. Hilt, "Formaldehyde," in *Ullmann's Encyclopedia of Industrial Chemistry*, I. F. Ullmann, W. Gerhartz, Y. S. Yamamoto, F. T. Campbell, R. Pfefferkorn, and J. F. Rounsaville, Eds., VCH, Deerfield Beach, FL, USA, 1985.

[8] H. R. Gerberich, A. L. Stautzenberger, and W. C. Hopkins, "Formaldehyde," in *Kirk-Othmer Encyclopaedia of Chemical Technology*, pp. 231–250, John Wiley and Sons, New York, 1980.

[9] E. Cao and A. Gavriilidis, "Oxidative dehydrogenation of methanol in a microstructured reactor," *Catalysis Today*, vol. 110, no. 1-2, pp. 154–163, 2005.

[10] K. I. Ivanov and D. Y. Dimitrov, "Deactivation of an industrial iron-molybdate catalyst for methanol oxidation," *Catalysis Today*, vol. 154, no. 3-4, pp. 250–255, 2010.

[11] K. Nakata, T. Ochiai, T. Murakami, and A. Fujishima, "Photoenergy conversion with TiO_2 photocatalysis: new materials and recent applications," *Electrochimica Acta*, vol. 84, pp. 103–111, 2012.

[12] K. Nakata and A. Fujishima, "TiO_2 photocatalysis: design and applications," *Journal of Photochemistry and Photobiology C: Photochemistry Reviews*, vol. 13, no. 3, pp. 169–189, 2012.

[13] S. Shamaila, A. K. L. Sajjad, F. Chen, and J. Zhang, "Synthesis and characterization of mesoporous-TiO_2 with enhanced photocatalytic activity for the degradation of chloro-phenol," *Materials Research Bulletin*, vol. 45, no. 10, pp. 1375–1382, 2010.

[14] C. P. Lin, H. Chen, A. Nakaruk, P. Koshy, and C. C. Sorrell, "Effect of annealing temperature on the photocatalytic activity of TiO_2 thin films," *Energy Procedia*, vol. 34, pp. 627–636, 2013.

[15] W. Dai, X. Wang, P. Liu, Y. Xu, G. Li, and X. Fu, "Effects of electron transfer between TiO_2 films and conducting substrates on the photocatalytic oxidation of organic pollutants," *The Journal of Physical Chemistry B*, vol. 110, no. 27, pp. 13470–13476, 2006.

[16] Y. Cui, J. Sun, Z. Hu et al., "Synthesis, phase transition and optical properties of nanocrystalline titanium dioxide films deposited by plasma assisted reactive pulsed laser deposition," *Surface and Coatings Technology*, vol. 231, pp. 180–184, 2013.

[17] X. Zhao, M. Liu, and Y. Zhu, "Fabrication of porous TiO_2 film via hydrothermal method and its photocatalytic performances," *Thin Solid Films*, vol. 515, no. 18, pp. 7127–7134, 2007.

[18] D. Li, M. Carette, A. Granier, J. P. Landesman, and A. Goullet, "In situ spectroscopic ellipsometry study of TiO_2 films deposited by plasma enhanced chemical vapour deposition," *Applied Surface Science*, vol. 283, pp. 234–239, 2013.

[19] A. Arunachalam, S. Dhanapandian, C. Manoharan, and R. Sridhar, "Characterization of sprayed TiO_2 on ITO substrates for solar cell applications," *Spectrochimica Acta Part A: Molecular and Biomolecular Spectroscopy*, vol. 149, pp. 904–912, 2015.

[20] A. Y. Shan, T. I. M. Ghazi, and S. A. Rashid, "Immobilisation of titanium dioxide onto supporting materials in heterogeneous photocatalysis: a review," *Applied Catalysis A: General*, vol. 389, no. 1-2, pp. 1–8, 2010.

[21] M. A. L. Vargas, M. Casanova, A. Trovarelli, and G. Busca, "An IR study of thermally stable V_2O_5-WO_3 -TiO_2 SCR catalysts modified with silica and rare-earths (Ce, Tb, Er)," *Applied Catalysis B: Environmental*, vol. 75, no. 3-4, pp. 303–311, 2007.

[22] W. Chang, L. Yan, Bin Liu, and R. Sun, "Photocatalyic activity of double pore structure TiO_2/SiO_2 monoliths," *Ceramics International*, vol. 43, no. 8, pp. 5881–5886, 2017.

[23] C. J. Brinker, "Hydrolysis and condensation of silicates: effects on structure," *Journal of Non-Crystalline Solids*, vol. 100, no. 1-3, pp. 31–50, 1988.

[24] G. Andrade-Espinosa, V. Escobar-Barrios, and R. Rangel-Mendez, "Synthesis and characterization of silica xerogels obtained via fast sol–gel process," *Colloid and Polymer Science*, vol. 288, no. 18, pp. 1697–1704, 2010.

[25] M. Ahmad, J. R. Jones, and L. L. Hench, "Fabricating sol–gel glass monoliths with controlled nanoporosity," *Biomedical Materials*, vol. 2, no. 1, pp. 6–10, 2007.

[26] Y. Farhang Ghoje Biglu and E. Taheri-Nassaj, "Investigation of phase separation of nano-crystalline anatase from TiO2-SiO2 thin film," *Ceramics International*, vol. 39, no. 3, pp. 2511–2518, 2013.

[27] S. Uchiyama, Y. Inaba, and N. Kunugita, "Derivatization of carbonyl compounds with 2,4-dinitrophenylhydrazine and their subsequent determination by high-performance liquid chromatography," *Journal of Chromatography B*, vol. 879, no. 17-18, pp. 1282–1289, 2011.

[28] M. S. Lee, S. S. Park, G. D. Lee, C. S. Ju, and S. S. Hong, "Synthesis of TiO_2 particles by reverse microemulsion method using nonionic surfactants with different hydrophilic and hydrophobic group and their photocatalytic activity," *Catalysis Today*, vol. 101, no. 3-4, pp. 283–290, 2005.

[29] R. Kaplan, B. Erjavec, G. Dražić, J. Grdadolnik, and A. Pintar, "Simple synthesis of anatase/rutile/brookite TiO_2 nanocomposite with superior mineralization potential for photocatalytic degradation of water pollutants," *Applied Catalysis B: Environmental*, vol. 181, pp. 465–474, 2016.

[30] Z. Fu, U. Eckstein, A. Dellert, and A. Roosen, "In situ study of mass loss, shrinkage and stress development during drying of cast colloidal films," *Journal of the European Ceramic Society*, vol. 35, no. 10, pp. 2883–2893, 2015.

[31] N. Arconada, A. Durán, S. Suárez et al., "Synthesis and photocatalytic properties of dense and porous TiO_2-anatase thin films prepared by sol–gel," *Applied Catalysis B: Environmental*, vol. 86, no. 1-2, pp. 1–7, 2009.

[32] C. M. Malengreaux, G. M. L. Léonard, S. L. Pirard et al., "How to modify the photocatalytic activity of TiO_2 thin films through their roughness by using additives. A relation between kinetics, morphology and synthesis," *Chemical Engineering Journal*, vol. 243, pp. 537–548, 2014.

[33] J. M. Stokke, D. W. Mazyck, C. Y. Wu, and R. Sheahan, "Photocatalytic oxidation of methanol using silica-titania composites in a packed-bed reactor," *Environmental Progress*, vol. 25, no. 4, pp. 312–318, 2006.